





Please cite the Published Version

Camargo, JR, Crapnell, RD , Bernalte, E, Cunliffe, AJ , Redfern, J , Janegitz, BC and Banks, CE  (2024) Conductive recycled PETg additive manufacturing filament for sterilisable electroanalytical healthcare sensors. *Applied Materials Today*, 39. 102285 ISSN 2352-9407

DOI: <https://doi.org/10.1016/j.apmt.2024.102285>

Publisher: Elsevier

Version: Published Version

Downloaded from: <https://e-space.mmu.ac.uk/635330/>

Usage rights:  [Creative Commons: Attribution 4.0](https://creativecommons.org/licenses/by/4.0/)

Additional Information: This is an open access article published in *Applied Materials Today*, by Elsevier.

Enquiries:

If you have questions about this document, contact openresearch@mmu.ac.uk. Please include the URL of the record in e-space. If you believe that your, or a third party's rights have been compromised through this document please see our Take Down policy (available from <https://www.mmu.ac.uk/library/using-the-library/policies-and-guidelines>)



Conductive recycled PETg additive manufacturing filament for sterilisable electroanalytical healthcare sensors

Jéssica R. Camargo^{a,b}, Robert D. Crapnell^a, Elena Bernalte^a, Alexander J. Cunliffe^a, James Redfern^a, Bruno C. Janegitz^b, Craig E. Banks^{a,*}

^a Faculty of Science and Engineering, Manchester Metropolitan University, Chester Street, M1 5GD, Great Britain

^b Laboratory of Sensors, Nanomedicine and Nanostructured Materials, Federal University of São Carlos, Araras 13600-970, Brazil

ARTICLE INFO

Keywords:

Additive manufacturing (3D-printing)
Sustainability
PETg
Uric acid
Sodium nitrite
Health care sensor

ABSTRACT

Current reports of healthcare sensors within literature that use additive manufacturing electrochemistry all utilise conductive PLA, which is unsuitable for widespread use within the industry. Poly(ethylene terephthalate glycol) (PETg) is a polymeric material with proven attributes for additive manufacturing due to its thermal and mechanical properties. Likewise, its excellent chemical stability transforms PETg into a desirable alternative for developing healthcare sensing devices. In this work, we report the production, physicochemical and electrochemical characterisations, as well as the electroanalytical performance of an enhanced electrically conductive additive manufacturing filament made with recycled poly(ethylene terephthalate glycol) (rPETg) and a combination of carbon black, multi-walled carbon nanotubes and graphene nanoplatelets as conductive fillers. The post-print activation of additive manufactured electrodes from this material is optimised and shown to produce enhanced electrochemical performance compared to non-activated electrodes, with a k^0 of $1.03 \times 10^{-3} \text{ cm s}^{-1}$. The sterilisation for the real application of sensors in the biomedical field is a critical point, the electrodes were submitted to standard UV light treatment showing to be reliable compared to PLA in the determination of uric acid (30–500 μM) and sodium nitrite (0.1–5 mM) within synthetic urine using differential pulse voltammetry and chronoamperometry techniques. A sensitivity and LOD for uric acid of $25.7 \mu\text{A } \mu\text{M}^{-1}$ and $0.27 \mu\text{M}$, and $52.6 \mu\text{A mM}^{-1}$ and $2.69 \mu\text{M}$ for nitrite were obtained within synthetic urine, respectively. The re-useability of the electrodes was also tested for the detection of uric acid, showing that the electrode could be used up to 10 times before a significant decrease in the results was observed. We demonstrate that a new conductive rPETg with superior electrochemical performance has a prominent place within the development of additive manufactured-printed healthcare sensors due to its ability to be sterilised and re-used, low solution ingress, and its potential to tackle rising costs and plastic waste problems within the healthcare sector.

1. Introduction

Additive manufacturing has become a staple tool within the electrochemists' arsenal as it allows for the production of parts on-demand with low (potentially zero) waste, rapid prototyping capabilities, a high degree of customisability, ease for global collaboration, and the ability to make complex geometries [1–4]. This is achieved through the simplified and local workplan of additive manufacturing, whereby a computer-aided design (CAD) file is created, and then processed into a physical 3D object through the application of consecutive, layered cross-sections of material onto a build platform. In particular, Fused Filament Fabrication (FFF) has been embraced by electrochemists due to

its relatively low-cost of entry, with both printers and printing material well within the budget of most research teams. FFF functions through the extrusion of a millimetre scale thermoplastic polymer through a nozzle heated to an appropriate temperature. The movement of the printer head then draws a thin cross-section of the molten polymer onto the print bed, or previously deposited layers, to build the 3-dimensional object once the polymer cools and solidifies. This manufacturing technique has been utilised within electrochemical labs for the production of bespoke accessories, equipment, electrochemical cells and electrodes of varying geometries [5–7].

To produce electrodes, electrically conductive filament must be used, of which there are a few commercially available options. The two most

* Corresponding author.

E-mail address: c.banks@mmu.ac.uk (C.E. Banks).

<https://doi.org/10.1016/j.apmt.2024.102285>

Received 22 March 2024; Received in revised form 4 June 2024; Accepted 7 June 2024

Available online 13 June 2024

2352-9407/© 2024 The Authors. Published by Elsevier Ltd. This is an open access article under the CC BY license (<http://creativecommons.org/licenses/by/4.0/>).

commonly used within the electrochemical literature both utilise poly (lactic acid) (PLA) as the base polymer, which is then filled with a conductive carbon to induce conductivity. Utilising these filaments, electrochemists have reported additively manufactured electrodes for use within energy applications [8–11] and electroanalysis, including for forensic [12–14], environmental [15–17], and biosensing applications [18–20]. Although the additive manufactured nature of these platforms offers its unique advantages, the electrochemical performance of many of these devices remains significantly inadequate compared to more classical electrodes. As such, there has recently been a push by some research groups to produce their own bespoke electrically conductive filament, with significantly greater conductivity than their commercially available counterparts. The base polymer for these filaments is commonly embedded with nanofillers through either solvent mixing or thermal mixing, with Crapnell and co-workers having recently reported a review on their production [21]. There are numerous recent examples of bespoke additive manufacturing filament, offering significantly enhanced electrochemical performance over the commercial alternative for energy applications [22,23], water electrolysis [24] and electroanalysis [25–31]. Recently, there has been an emphasis placed on improving the sustainability of these filaments, with Sigley and co-workers first reporting the use of recycled PLA to produce conductive filaments for the electroanalytical detection of caffeine [32]. Following this, Crapnell and co-workers showed that used electroanalytical sensors could be recycled into filament and re-used to create identical sensing platforms [33], and then also showed how the plasticiser used to create conductive filament could be changed to bio-based castor oil, whilst still producing filament with excellent conductivity and low-temperature flexibility [34].

Although these bespoke filaments all show excellent electrochemical performance, they are all still utilising PLA as the base polymer for filament production and are therefore limited by the physicochemical properties provided by PLA. It has been shown that over multiple years the electrochemical performance of conductive PLA deteriorates, even with proper storage [35]. Additionally, ingress of water is a significant issue with regards to PLA-based additive manufactured electrodes, showing an increase in mass of 1–1.5 % and a subsequent reduction in the measured peak currents [36]. Finally, PLA offers some of the worst chemical resistances out of the commonly available additive manufacturing feedstocks [37], meaning that additive-manufactured electrodes made from these feedstocks will always have somewhat limited applications.

PETg, a glycol-modified PET (polyethylene terephthalate) copolymer has found a great amount of applications within the additive manufacturing field, with special emphasis in the FFF process, due to its excellent thermoforming, layer adhesion, and comparatively low-cost [38]. Like its precursor, PETg presents an excellent chemical resistance, good tensile toughness, flexibility and transparency, making of PETg another fantastic candidate for additive manufacturing applications. For example, reinforced PETg with carbon fibers or graphene has been proven satisfactory in engineering applications [39]. Also, due to its unique characteristics as a biomaterial, PETg has been actively applied in modern medicine, such as tissue engineering [40], dental, cardiovascular, pharmaceutical and surgical related applications [41]. Recently, it has been reported for the first time the fabrication of electrically conductive PETg to overcome some drawbacks found for PLA in electrochemical sensing applications, paving the way for novel applications of this material as electrochemical devices. [42]. In this work, the authors used recycled PETg with a combination of conductive nanomaterials to produce a filament with a total filler loading of 30 wt %. In this case, a base amount of carbon black (CB, 25 wt%) was combined with graphene nanoplatelets (GNPs, 2.5 wt%) and multi-walled carbon nanotubes (MWCNT, 2.5 wt%), with the work showing that the combination of all three nanomaterials provided a significantly improvement over loading with only 30 wt% carbon black or incorporating 5 wt% of a single additional nanomaterial. The combining of

nanomaterials to create an additive manufacturing filament with improved conductivity and electrochemical performance has also been seen previously for PLA based filaments, where combining MWCNT and carbon black produced a high performance sensors for acetaminophen and phenylephrine [27]. For the PETg filament mentioned above, the authors compared the electrochemical performance to the commonly used commercial conductive PLA and showed that it could match the performance. However, this means that the electrochemical performance of this filament is still some way off that of the bespoke PLA filaments that have been reported.

In the present work, we look to produce an electrically conductive recycled PETg (rPETg) with enhanced conductivity compared to previously reported by increasing in 5 % the total carbon loading in the filament without additional plasticiser. We aim to further improve the electrochemical performance of the additive manufactured-printed electrodes produced with the new filament through the optimisation of a mechanical activation procedure. We then look to exploit the advantageous chemical properties of PETg compared to PLA by investigating the feasibility of using both platforms in healthcare settings while detecting critical analytes in urine after electrodes undergoing standard UV sterilisation. Finally, we will look at the re-use of these electrodes to reduce the amount of plastic healthcare waste, which will, in turn, increase the chances of additive manufactured healthcare sensors becoming commercially realised.

2. Experimental

2.1. Chemicals

All chemicals used were of analytical grade and used as received without any further purification. All solutions were prepared with deionised water of resistivity not less than 18.2 M Ω cm from a Milli-Q Integral 3 system from Millipore UK (Watford, UK). Hexaamineruthenium (III) chloride (98 %), potassium ferricyanide (99 %), potassium ferrocyanide (98.5–102 %), sodium hydroxide (>98 %), potassium chloride (99.0–100.5 %), graphene nanoplatelets (>95 wt%), uric acid (99 %), sodium nitrite (\geq 99 %) and phosphate-buffered saline (PBS) tablets were purchased from Merck (Gillingham, UK). Acetone (\geq 99 %), acetonitrile (\geq 99.9 %), chloroform (\geq 99 %), dimethyl formamide (99+%), and tetrahydrofuran (99.8 %) were purchased from Fisher Scientific UK (Loughborough, UK). Carbon black (CB, C—NERGY Super C65) was purchased from PI-KEM (Tamworth, UK). Multi-walled carbon nanotubes (MWCNT, 10–30 μ m length, 10–20 nm outer diameter, >95 wt% purity) were purchased from Cheap Tubes (VT, United States). Recycled PETg was obtained from old lab prints, originally printed from Multicomp Pro PETG Natural 3D (1.75 mm) printer filament, which was purchased from Farnell (Leeds, UK) along with commercial conductive PLA/carbon black filament (1.75 mm, ProtoPasta, Vancouver, Canada).

2.2. Recycled filament production

Prior to any mixing or filament production, all rPETg was dried in an oven at 60 °C for a minimum of 2.5 h, which removed any residual water in the polymer. The polymer composition was prepared using 67 wt% rPETg and 33 wt% conductive filler. The conductive filler was split equally between the three constituents, 11 wt% carbon black, 11 wt% multi-walled carbon nanotubes and 11 wt% graphene nanoplatelets. The components were added into a chamber of 63 cm³ [3] and mixed at 230 °C with Banbury rotors at 70 rpm for 5 min using a Thermo Haake Poydrive dynamometer fitted with a Thermo Haake Rheomix 600 (Thermo-Haake, Germany). The resulting polymer composite was allowed to cool to room temperature before being granulated to create a finer granule size using a Rapid Granulator 1528 (Rapid, Sweden). The collected and processed through the hopper of an EX6 extrusion line (Filabot, VA, United States). The EX6 was set up with a single screw and had four set heat zones of 60, 230, 230 and 235 °C respectively. The

molten polymer was extruded from a 1.75 mm die head, pulled along an Airpath cooling line (Filabot, VA, United States, through an inline measure (Mitutoyo, Japan) and collected on a Filabot spooler (Filabot, VA, United States). The filament was then ready to use for additive manufacturing.

2.3. Additive manufacturing

All computer designs and .3MF files seen throughout this manuscript were produced using Fusion 360® (Autodesk®, CA, United States). These files were sliced and converted to GCODE files ready for printing by the open-source software, PrusaSlicer (Prusa Research, Prague, Czech Republic). The additive manufacturing electrodes were 3D-printed using fused filament fabrication (FFF) technology on a Prusa i3 MK3S+ (Prusa Research, Prague, Czech Republic). All additive manufacturing electrodes were printed using a 0.6 mm nozzle with a nozzle temperature of 250 °C, 100 % rectilinear infill [43], 0.15 mm layer height, and print speed of 35 mm s⁻¹. All additive manufactured electrodes used throughout this work were “lollipop” designs with a 5 mm disc, 8 × 2 mm connection stem and 1 mm thick. In all cases, polyimide tape was placed on top of the print bed as PETg can cause damage upon removal due to the strength of adhesion.

2.4. Activation procedures

Activation of the additive manufactured electrodes was performed in different ways. For solvent activation, the electrode was placed within a vial of the solvent and sonicated for 10 min before being washed with deionised water and dried thoroughly before use.

Mechanical activation was performed initially using emery paper (800 grit) (3 M, Bracknell, UK). Mechanical polishing was performed using a Dremel® Model 200 Multi-Tool with 4 sanding accessories (pictured in the SI).

Electrochemical activation of the additive manufactured electrodes was performed in NaOH, as described in the literature [44]. Briefly, the additive manufactured electrodes were connected as the working electrode in conjunction with a nichrome wire coil counter and Ag|AgCl (3 M KCl) reference electrode and placed in a solution of NaOH (0.5 M). Chronoamperometry was used to activate the additive manufactured electrodes by applying a set voltage of + 1.4 V for 200 s, followed by applying - 1.0 V for 200 s. The additive manufactured electrodes were then thoroughly rinsed with deionised water and dried under compressed air before further use.

2.5. Physicochemical characterisation

X-ray Photoelectron Spectroscopy (XPS) data were acquired using an AXIS Supra (Kratos, UK), equipped with a monochromated Al X-ray source (1486.6 eV) operating at 225 W and a hemispherical sector analyser. It was operated in fixed transmission mode with a pass energy of 160 eV for survey scans and 20 eV for region scans with the collimator operating in slot mode for an analysis area of approximately 700×300 µm, the FWHM of the Ag 3d5/2 peak using a pass energy of 20 eV was 0.613 eV. Before analysis, each sample was ultrasonicated for 15 min in propan-2-ol and then dried for 2.5 h at 65 °C as shown in our unpublished data to remove excess contamination and minimise the risk of misleading data. Baseline correction was performed using the Shirley background, the graphitic peaks were fitted using an asymmetric peak and the other carbon peaks were fitted using symmetric peaks. The binding energy scale was calibrated by setting the graphitic sp² C 1s peak to 284.5 eV; this calibration is acknowledged to be flawed [45] but was nonetheless used in the absence of reasonable alternatives, and because only limited information was to be inferred from absolute peak positions.

Scanning Electron Microscopy (SEM) micrographs were obtained using a Crossbeam 350 Focussed Ion Beam – Scanning Electron

Microscope (FIB-SEM) (Carl Zeiss Ltd., Cambridge, UK) fitted with a field emission electron gun. Imaging was completed using a Secondary Electron Secondary Ion (SESI) detector. Samples were mounted on the aluminium SEM pin stubs (12 mm diameter, Agar Scientific, Essex, UK) using adhesive carbon tabs (12 mm diameter, Agar Scientific, Essex, UK) and coated with a 3 nm layer of Au/Pd metal using a Leica EM ACE200 coating system before imaging.

Raman spectroscopy was performed on a Renishaw PLC in Via Raman Microscope controlled by WiRE 2 software at a laser wavelength of 514 nm between 3000 and 100 cm⁻¹. Performed with a laser power of 2 mW, 20 sample exposures, and a lateral resolution of 1 µm.

2.6. Electrochemical experiments

All electrochemical measurements were performed on an Autolab 100 N potentiostat controlled by NOVA 2.1.6 (Utrecht, the Netherlands). The electrochemical characterisation of the bespoke filament and comparison to the benchmarks were performed using a lollipop design (Ø 5 mm disc with 8 mm connection length and 2 × 1 mm thickness) electrodes alongside either an external commercial Ag|AgCl (3 M KCl) reference electrode with a nichrome wire counter electrode or an additive manufactured reference electrode with an AM counter electrode. All solutions of Hexaamineruthenium (III) chloride were prepared using deionised water of resistivity not less than 18.2 MΩ cm from a Milli-Q system (Merck, Gillingham, UK) and were purged of O₂ thoroughly using N₂ before any electrochemical experiments.

2.7. Sterilisation and microbiology experiments

To sterilise the additive manufactured electrodes, they were placed within an Anycubic Wash and Cure Plus station and irradiated with UV light for 4 h. Following irradiation, electrodes were aseptically transferred to individual 30 mL sterile universal tubes containing 10 mL of sterile Tryptone Soya Broth (TSB, Oxoid, UK), that had been prepared following manufacturers requirements. Each tube was incubated, shaking at 150 rpm (50 mm throw), at 37 °C (optimal temperature for human bacterial pathogens to grow) for 18 h. Each tube was then assessed for the presence of microbial growth (as indicated by TSB turning cloudy).

3. Results and discussion

In previous work, it was shown that the addition of 2.5 wt% MWCNT and 2.5 wt% GNPs in combination with 25 wt% CB was adequate nanocarbon incorporation to produce an electrically conductive additive manufacturing filament from rPETg that gave similar electrochemical performance to the commercially available conductive PLA commonly used throughout the electrochemical literature [42]. The rPETg filament was activated using the chronoamperometric method within aqueous sodium hydroxide (0.5 M), which is well-established for PLA [44]. However, there have been many other methods trialled for PLA, and therefore we will look to explore alternative methods to improve the performance of conductive rPETg toward inner-sphere probes. To further improve on the conductivity of the rPETg and the electrochemical performance of the additive manufactured electrodes produced from this filament, we look to further increase the loadings of MWCNT and GNPs in line with CB, resulting in a filament containing 11 wt% of each material, leading to an overall 3 wt% increase in total nanocarbon filler. We found that this overall loading of 33 wt% was the maximum that could be achieved through thermal mixing methodology within our rPETg polymer, without the addition of a further plasticiser compound. Combinations of carbon allotropes with different morphologies has been seen within previous work to improve the conductive network through the native insulating materials [27,42,46]. It is important to understand the morphologies and characteristics of the materials used, even if they are commercially purchased due to possible

batch to batch variations. Fig. S1 A–C provides SEM images of the three carbon powders used within this work, where the morphologies can be seen. Carbon black is present as nanometre scale spherical particles, graphene nanoplatelets as larger sheets and the multiwalled carbon nanotubes as long, narrow tubes. The Raman spectra for each of these powders is found in Fig. S1 D–F, where in all three cases the characteristic intense peaks of graphitic-like structures at 1338, 1572, and 2680 cm^{-1} are present and assigned to the D-, G-, and 2D-bands respectively. It is noticeable that the G-band within the graphene sample is significantly larger than the D-band, indicating a high degree of order and a low number of structural defects. Understanding these individual structures will help understand the filament when all are combined.

3.1. Activation of PETg for improved electrochemical performance

When utilising additive manufactured electrodes, it has been seen that activating the electrode is often required for adequate electrochemical performance against inner-sphere redox probes. This is due to a “gloving” effect upon filament extrusion which leaves a polymeric layer on the surface of the print embedding the conductive nanofillers below. This phenomenon has been confirmed for both PETg and PLA in previous works [12,25,26,34,44], and although some bespoke PLA filaments show good electrochemical performance as printed, it has been shown that activation still improves the performance of these platforms [27,32]. For PLA, there has been extensive work looking at different activation methodologies [47,48]; however, for the previously reported conductive rPETg only electrochemical activation within aqueous sodium hydroxide (0.5 M) was considered. Fig. 1 shows cyclic voltammograms (25 mV s^{-1}) in $[\text{Fe}(\text{CN})_6]^{4-/3-}$ (1 mM in 0.1 M KCl) using additive manufactured electrodes printed from the new conductive rPETg after various treatments, including simple polishing using emery paper, electrochemical activation, and sonication within acetone, acetonitrile, chloroform, DMF, and THF. These solvents were chosen due to PETg’s poor stability within them [37], therefore their expected capability to remove PETg from the surface of the print. It can be seen however that the best performances are obtained for simply polishing the electrode with emery paper or for electrochemically activating it within aqueous sodium hydroxide (0.5 M).

After establishing that polishing the electrode significantly improved the electrochemical performance, the ability to provide a reproducible finish using a polishing machine was sought. Fig. S2A provides an

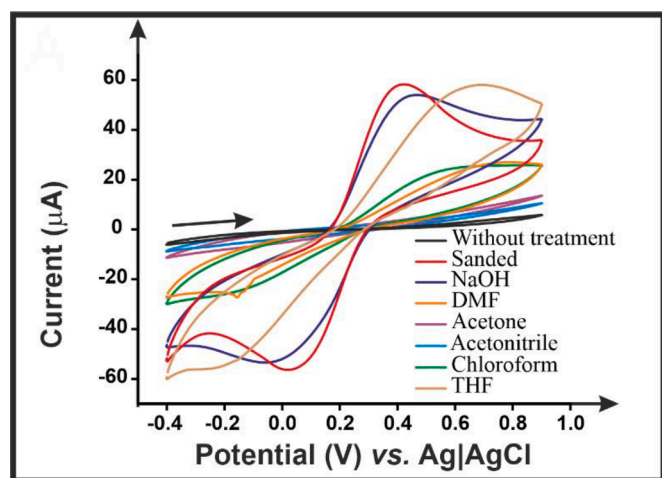


Fig. 1. Cyclic voltammograms (25 mV s^{-1}) in $[\text{Fe}(\text{CN})_6]^{4-/3-}$ (1 mM in 0.1 M KCl) using additive manufactured electrodes printed from the developed rPETg filament untreated and treated through soaking within the named solvent for 10 min, or through sanding (800 grit) with emery paper with a nichrome coil counter electrode, and Ag|AgCl as the reference electrode.

overview of the different mechanical polishing heads used, with Fig. S2B showing that the second machine head provided the best response within $[\text{Fe}(\text{CN})_6]^{4-/3-}$ (1 mM in 0.1 M KCl). Following this, it was tested whether polishing the entire electrode or only the head and connection would produce the best result. Fig. 2A clearly shows that the best response was obtained through only polishing the head, where the electrochemical reaction occurs, and the connection where the crocodile clip is placed.

Finally, a combination of both polishing followed by electrochemically activating the additive manufactured electrode was tested. Fig. 2B presents the cyclic voltammograms (25 mV s^{-1}) obtained within $[\text{Fe}(\text{CN})_6]^{4-/3-}$ (1 mM in 0.1 M KCl) for both these cases, which clearly shows an improvement in electrochemical performance when combining both activation procedures. This procedure was therefore chosen to be used throughout the rest of this work.

3.2. Physicochemical characterisation of bespoke PETg electrodes

It is important to establish what effect this activation procedure has on the surface of the additive manufactured electrode. Fig. 3A presents the XPS C 1s spectra for the as printed additive manufactured electrode, with the only polished spectra presented in Fig. S3 and the polished and electrochemically activated spectra in Fig. 3B. For the as-printed electrode, the XPS spectra show good agreement with that published previously [42], utilising three symmetric peaks fitted for the C-C, C-O and O-C=O bonding found within PETg, with the C-C peak showing a much higher intensity [49]. For adequate fitting, an asymmetric peak is also required at 284.5 eV, which is consistent with the X-ray photoelectron emission by graphitic carbon [50,51]. This graphitic carbon peak is small, accounting for only 5 % of the composition, which indicates that the majority of the conductive carbon is not available on the surface of the electrode. In contrast, both the only polished and polished with electrochemical activation additive manufactured electrodes showed a large increase in the asymmetric graphitic peak, with the atomic concentration increasing from ~5 % up to ~40 % in both activated samples, see Table S1. This level of increase in the graphitic carbon peak is indicative of the exposure of significant amounts of nanocarbon that was previously embedded below the polymer. When compared to the previous report of rPETg which only utilised electrochemical activation, an increase of only 4 % was seen in the graphitic carbon peak, indicating this methodology is a vast improvement. It is inferred that only electrochemical activation that was used in previous reports [42] only creates minor perforations on the surface of the electrode. In contrast the very abrasive nature of mechanical polishing significantly removes surface polymer, leaving the remaining polymer much more susceptible to attack.

To further confirm the presence of increased amounts of the nanocarbon on the surface of the additive manufactured electrode after activation, Raman analysis was performed. The as-printed and only polished spectra are presented in Fig. S4A and B, respectively, with the polished and electrochemically activated spectra shown in Fig. 3C. In all cases, the characteristic intense peaks of graphitic-like structures at 1338, 1572, and 2680 cm^{-1} are present and assigned to the D-, G-, and 2D-bands respectively. It can be seen that there is a clear increase in the G-band intensity for the additive manufactured electrode after both polishing and electrochemical activation with the I_D/I_G ratio decreasing from 0.8 to 0.47 (the only polished electrode gave a value of 0.8), indicating fewer defects and a more ordered structure as more GNPs and MWCNTs are exposed.

The additive manufactured electrodes were then analysed using SEM, where the images are presented in Fig. 3D–F. In all cases the different carbon morphologies can be seen, with the CB presenting as spherical clumps, the MWCNT being long thin structures, and the GNPs being expansive flakes, consistent with the SEM images obtained for the powders in Fig. S1. On the as printed electrode, Fig. 3D, there is a clear covering of polymer on the surface and in between the nanocarbons, and

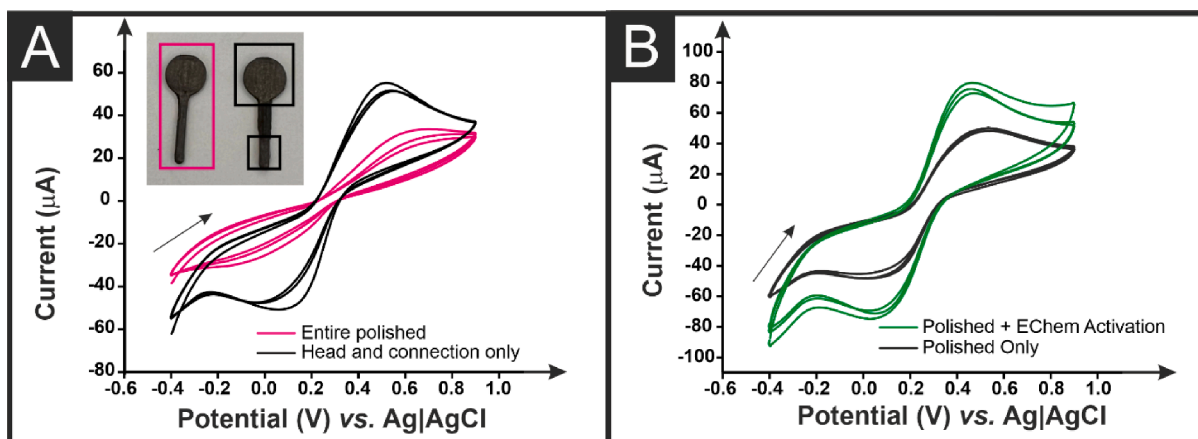


Fig. 2. (A) Cyclic voltammograms (25 mV s^{-1}) in $[\text{Fe}(\text{CN})_6]^{4-/3-}$ (1 mM in 0.1 M KCl) for working electrodes fully polished (pink) and only polished on the head and connection (black), with a nichrome wire counter electrode and Ag|AgCl reference electrode. (B) Cyclic voltammograms (25 mV s^{-1}) in $[\text{Fe}(\text{CN})_6]^{4-/3-}$ (1 mM in 0.1 M KCl) for working electrodes polished (black) versus polished and electrochemically activated (green), with a nichrome wire counter electrode and Ag|AgCl reference electrode.

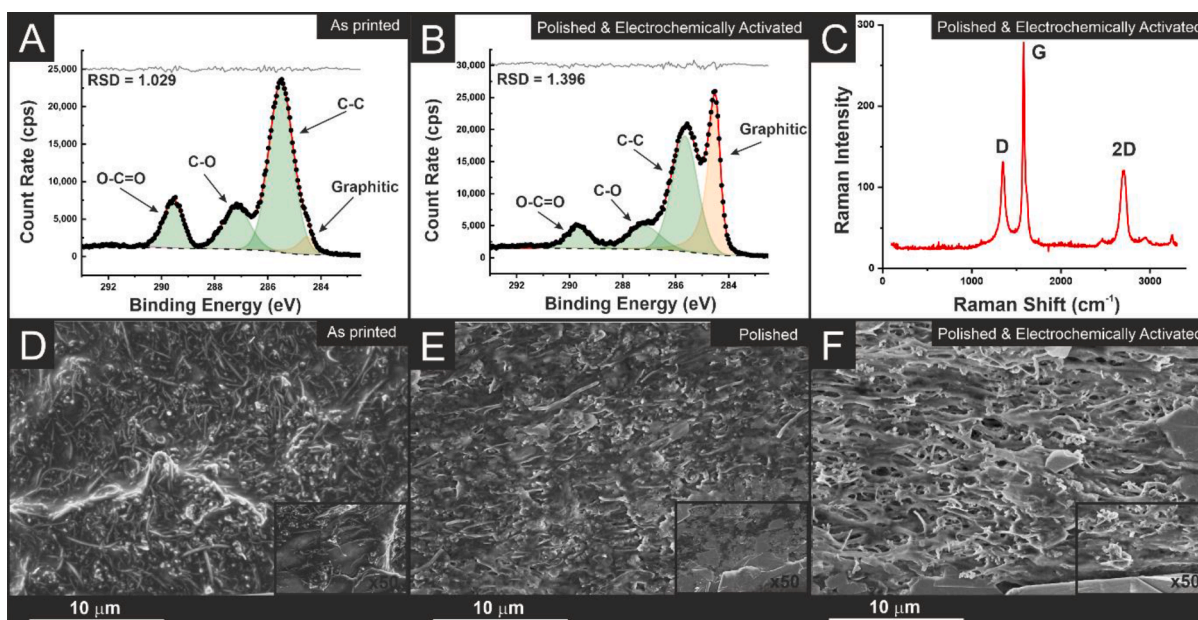


Fig. 3. XPS C 1s spectra for the (A) as printed and (B) polished and electrochemically activated additive manufactured electrodes printed from the rPETg filament. (C) Raman spectra obtained for the polished and electrochemically activated additive manufactured electrodes printed from the rPETg filament. SEM micrographs for the (D) as printed, (E) polished, and (F) polished and electrochemically activated additive manufactured electrodes printed from the rPETg filament at different magnifications.

even though their morphologies are visible, the XPS results above indicate a covering of at least a few nm of polymer. In the case of the polished electrode, Fig. 3E, there is clearly alignment of the nanocarbons caused through the mechanical polishing, which is most clear when considering the MWCNT which are now aligned horizontally, whereas in the as-printed sample, they have a random orientation. Interestingly, for the polished and electrochemically activated sample, Fig. 3F, there is the appearance of obvious voids in between the nanocarbon structures which are not seen in the other samples. This indicates that after the polishing, the additional electrochemical activation removes significant amounts of polymer exposing more the nanocarbon structures. When compared to the SEM images in previous work for electrochemically activated PETg only small and sporadic surface voids were formed, indicating that the combination of polishing and electrochemical activation results in the removal of significantly more surface polymer.

3.3. Electrochemical performance of bespoke rPETg electrodes

Initially, this filament was tested through scan rate studies using an untreated additive manufactured electrode against the near-ideal outer sphere redox probe $[\text{Ru}(\text{NH}_3)_6]^{3+/2+}$ (1 mM, in 0.1 M KCl, Fig. 4A, which allowed for the best determination of the heterogeneous electrochemical rate constant (k^0) and the real electrochemical surface area (A_e) [52].

Through scan rate studies against $[\text{Ru}(\text{NH}_3)_6]^{3+/2+}$ using additive manufactured electrodes of the same dimensions, but printed from different materials a direct comparison between the new rPETg in this work, the previously reported conductive rPETg, and the commercially available benchmark PLA can be achieved. Fig. 4B exhibits this comparison using cyclic voltammograms (100 mV s^{-1}) within $[\text{Ru}(\text{NH}_3)_6]^{3+/2+}$ (1 mM, in 0.1 M KCl), which clearly show an improvement in terms of the peak reduction current and peak-to-peak separation for

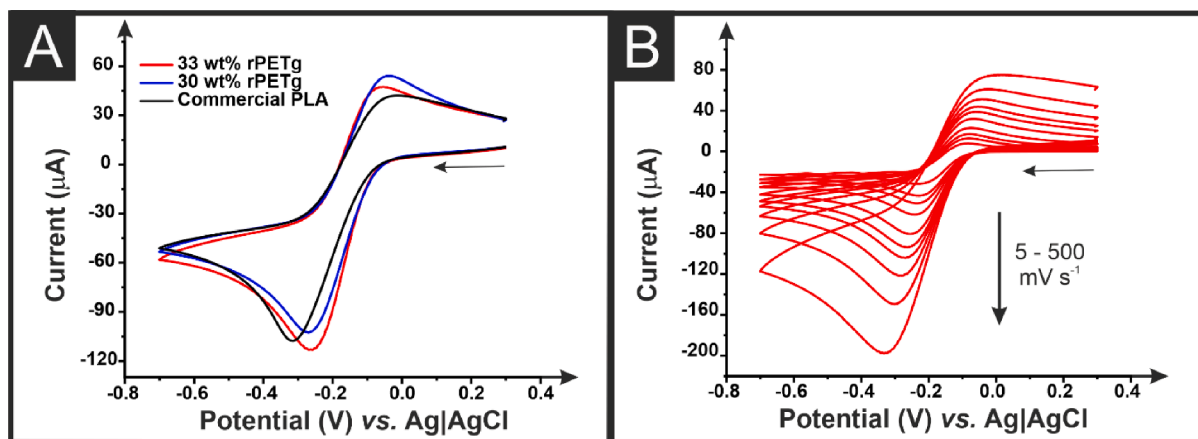


Fig. 4. (A) Cyclic voltammograms (100 mV s^{-1}) in $[\text{Ru}(\text{NH}_3)_6]^{3+/2+}$ (1 mM in 0.1 M KCl) performed with additive manufactured electrodes printed from the rPETg filament (11 wt% CB, 11 wt% MWCNT, 11 wt% GNPs) from this work (red line), the rPETg filament (25 wt% CB, 2.5 wt% MWCNT, 2.5 wt% GNPs) previously reported (blue line), and a commonly used commercial conductive PLA filament (black line) as the working electrodes, nichrome coil and a Ag|AgCl (3 M KCl) as counter and reference electrode, respectively. (B) Scan rate study ($5\text{--}500 \text{ mV s}^{-1}$) in $[\text{Ru}(\text{NH}_3)_6]^{3+}$ (1 mM in 0.1 M KCl) performed with the rPETg (11 wt% CB, 11 wt% MWCNT, 11 wt% GNPs) additive manufactured electrode as the working electrode, nichrome coil counter electrode, and Ag|AgCl (3 M KCl) reference electrode, respectively.

the new rPETg filament. This translates into the calculated k^0 values, where the new rPETg filament produced a value of $1.03 \times 10^{-3} \text{ cm s}^{-1}$, compared to $8.82 \times 10^{-4} \text{ cm s}^{-1}$ for the previous conductive rPETg and $4.57 \times 10^{-4} \text{ cm s}^{-1}$ for the conductive commercial PLA. This highlights how the conductivity and electrochemical performance of the new rPETg filament is significantly improved when compared to the old rPETg filament and the commercial PLA. This filament is compared to other bespoke filaments reported in the literature within Table S2, where it can be seen that the filament is giving a good performance whilst also bringing the beneficial properties of PETg compared to PLA.

Finally, the polished and electrochemically activated electrode was utilised in a scan rate study with the inner-sphere probe $[\text{Fe}(\text{CN})_6]^{4-/3-}$ (1 mM in 0.1 M KCl), where Fig. S5A shows the excellent inter-electrode reproducibility and Fig. S5B shows the cyclic voltammograms obtained in the scan rate study. Using this activation procedure, we now turn toward the electroanalytical application for this new rPETg filament.

3.4. Sterilisation and electroanalytical application

For the realistic uptake of additive manufactured electrochemical platforms into healthcare settings, the electrodes must be sterilisable and still give a reliable electrochemical performance. In previous work it was shown that conductive rPETg was able to be sterilised using an alcoholic solution and still produce reproducible results. Herein we look to show its ability to perform after sterilisation through exposure to UV light on a standard benchtop setting. To achieve this, additive manufactured electrodes were printed and then sterilised using a post-printing UV curing machine, typically utilised for stereolithography prints. To ensure the successful nature of the sterilisation procedure, triplicates of these electrodes were incubated within growth media for 18 h. Images of the solutions after incubation can be seen in Fig. S6, where all of the as-printed electrodes resulted in a cloudy suspension, indicating significant bacteria growth. In comparison all of the additive manufactured electrodes that were treated with UV resulted in a clear suspension, providing evidence of the successful sterilisation of the electrodes. This sterilisation methodology was used on additive manufactured electrodes printed from the rPETg, and from the commercially available conductive PLA as a comparison. Once sterilised these electrodes were used for the detection of uric acid (100 μM) within a solution of Britton-Robinson buffer (pH 5.0). Fig. 5A presents the results for rPETg additive manufactured electrodes as printed, and after 2 and 4 h of UV treatment, with

Fig. 5B showing the corresponding results for the sterilised commercial PLA electrodes. It can be seen that the rPETg additive manufactured electrodes show no deviation in the electroanalytical response toward uric acid after either sterilisation time. In comparison, the PLA additive manufactured electrodes show a significant instability in the peak potentials and a clear increase in the peak current after 2 h of UV treatment and then a slight reduction after 4 h. Although this could indicate an interesting way to activate PLA additive manufactured electrodes in the future it raises severe concerns about the reliability of using PLA based electrodes in this setting.

The rPETg additive manufactured electrodes were then applied toward the electroanalytical detection of uric acid and sodium nitrite within Britton-Robinson buffer (pH 5.0). For these studies differential pulse voltammetry (DPV) was utilised for the detection of uric acid and chronoamperometry was used for the detection of sodium nitrite, highlighting the flexibility of these additive manufactured electrodes. Fig. 5C exhibits the DPV results for the determination of uric acid (30–500 μM), where two linear ranges were observed on the calibration plot inset. The first between 30 and 100 μM , with an equation $I = 0.02969 [\text{Uric Acid}] - 5.98563 \times 10^{-7}$, provided a sensitivity of $29.7 \mu\text{A } \mu\text{M}^{-1}$, a limit of quantification (LOQ) of $0.44 \mu\text{M}$, and a limit of detection (LOD) of $0.13 \mu\text{M}$. The second linear range was observed between 100 and 500 μM , with an equation $I = 0.00894 [\text{Uric Acid}] - 2.02052 \times 10^{-6}$ exhibited a sensitivity of $8.9 \mu\text{A } \mu\text{M}^{-1}$ a limit of quantification (LOQ) of $1.46 \mu\text{M}$, and a limit of detection (LOD) of $0.43 \mu\text{M}$. The LOD are comparable to additive manufactured sensors reporting $0.07 \mu\text{M}$ using graphite-PLA[53] and $0.02 \mu\text{M}$ using graphene-PLA [54]. Fig. 5D shows the chronoamperometric response to the determination of sodium nitrite (0.1–5 mM), where a single linear response, with an equation $I = 0.01994 [\text{sodium nitrite}] + 6.87 \times 10^{-6}$, was observed in the calibration plot inset with an R^2 value of 0.9938. This plot was used to calculate the sensitivity of $19.9 \mu\text{A mM}^{-1}$, LOQ of $10.6 \mu\text{M}$ and LOD of $3.16 \mu\text{M}$.

One advantage of utilising rPETg seen previously [42] is the minimal solution ingress and ability to re-use the additive manufactured electrodes with reliable results. This was then tested for the determination of uric acid through cyclic voltammetry, Fig. 5E, whereby the additive manufactured electrode was used, washed, re-activated within aqueous sodium hydroxide, and dried before re-use. This was performed for 20 repeat cycles, with the results in terms of peak current represented in Fig. 5F. It can be seen that for the first 10 measurements, there is excellent agreement between the obtained values, after which there is a reduction in the measured peak current. This indicates the ability to

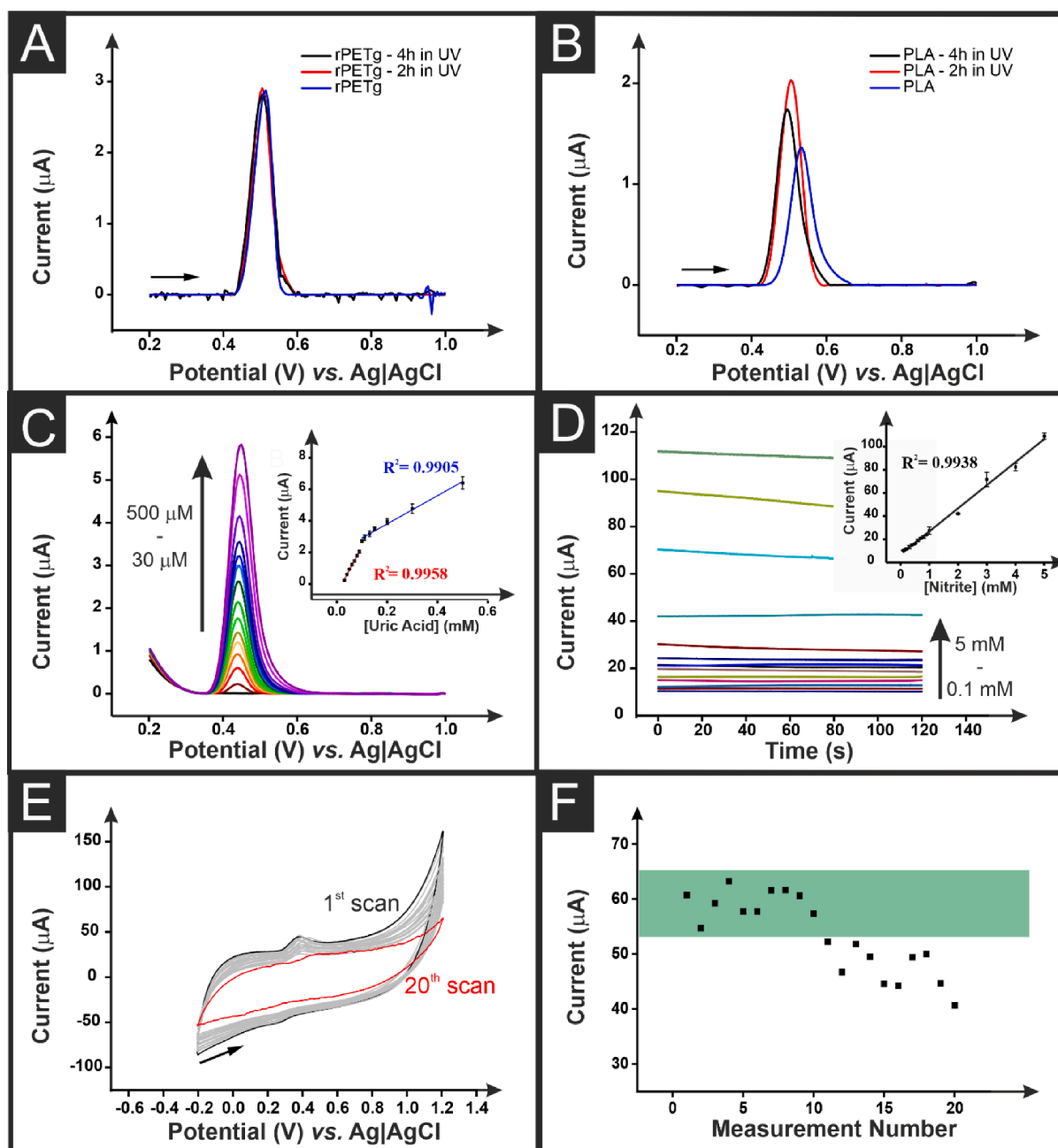


Fig. 5. Differential pulse voltammograms of uric acid ($100\ \mu\text{M}$) in $0.1\ \text{M}$ Britton-Robinson buffer ($\text{pH}\ 5.0$) using sterilised additive manufactured electrodes printed from (A) the rPETg additive manufactured electrode and (B) a commercial PLA additive manufactured electrode, nichrome wire counter electrode and Ag|AgCl reference electrode. Differential pulse voltammograms conditions: step potential of $5\ \text{mV}$, amplitude of $25\ \text{mV}$, modulation time of $50\ \text{s}$, and interval time of $0.5\ \text{s}$. (C) Differential pulse voltammograms of uric acid ($30\text{--}500\ \mu\text{M}$) in $0.1\ \text{M}$ Britton-Robinson buffer ($\text{pH}\ 5.0$) using the rPETg additive manufactured electrode, nichrome wire counter electrode and Ag|AgCl reference electrode. Performed with a step potential of $5\ \text{mV}$, amplitude of $25\ \text{mV}$, modulation time of $50\ \text{s}$, and interval time of $0.5\ \text{s}$. Calibration plot inset. (D) Chronoamperograms for the detection of sodium nitrite ($0.1\text{--}5\ \text{mM}$) in $0.1\ \text{M}$ Britton-Robinson buffer ($\text{pH}\ 5.0$) using the rPETg additive manufactured electrode, nichrome wire counter electrode and Ag|AgCl reference electrode. Calibration plot inset. (E) Cyclic voltammograms ($50\ \text{mV}\ \text{s}^{-1}$, $n = 20$) of uric acid ($0.1\ \text{mM}$) performed using the rPETg additive manufactured electrode, nichrome wire counter electrode and Ag|AgCl reference electrode. (F) Plot of the evolution of peak current versus the measurement number for the cyclic voltammograms obtained in E.

re-use the rPETg additive manufactured electrode a significant amount of times before deterioration, which could lead to significant cost savings. Finally, the sterilised rPETg additive manufactured electrodes were applied to the detection of these analytes within synthetic urine samples to highlight their real-world applicability.

The DPV response of the sterilised rPETg additive manufactured electrodes toward the detection of uric acid within a synthetic urine sample are presented with Fig. 6A, with the corresponding calibration plot shown in Fig. 6B. It can be seen that a response was observed

over similar concentration ranges as within buffered solution, with once again two linear ranges obtained. The first linear range ($30\text{--}100\ \mu\text{M}$) produced a sensitivity of $25.7\ \mu\text{A}\ \mu\text{M}^{-1}$, which is slightly lower than observed in solely buffered solution and can be attributed to matrix effects. Using this, the LOD and LOQ were calculated to be $0.27\ \mu\text{M}$ and $0.92\ \mu\text{M}$, respectively. The second linear range ($100\text{--}500\ \mu\text{M}$), exhibited a sensitivity of $9.8\ \mu\text{A}\ \mu\text{M}^{-1}$ a limit of quantification (LOQ) of $0.73\ \mu\text{M}$, and a limit of detection (LOD) of $2.42\ \mu\text{M}$. The chronoamperometric response to the detection of nitrite ($0.1\text{--}5\ \text{mM}$) within synthetic urine is

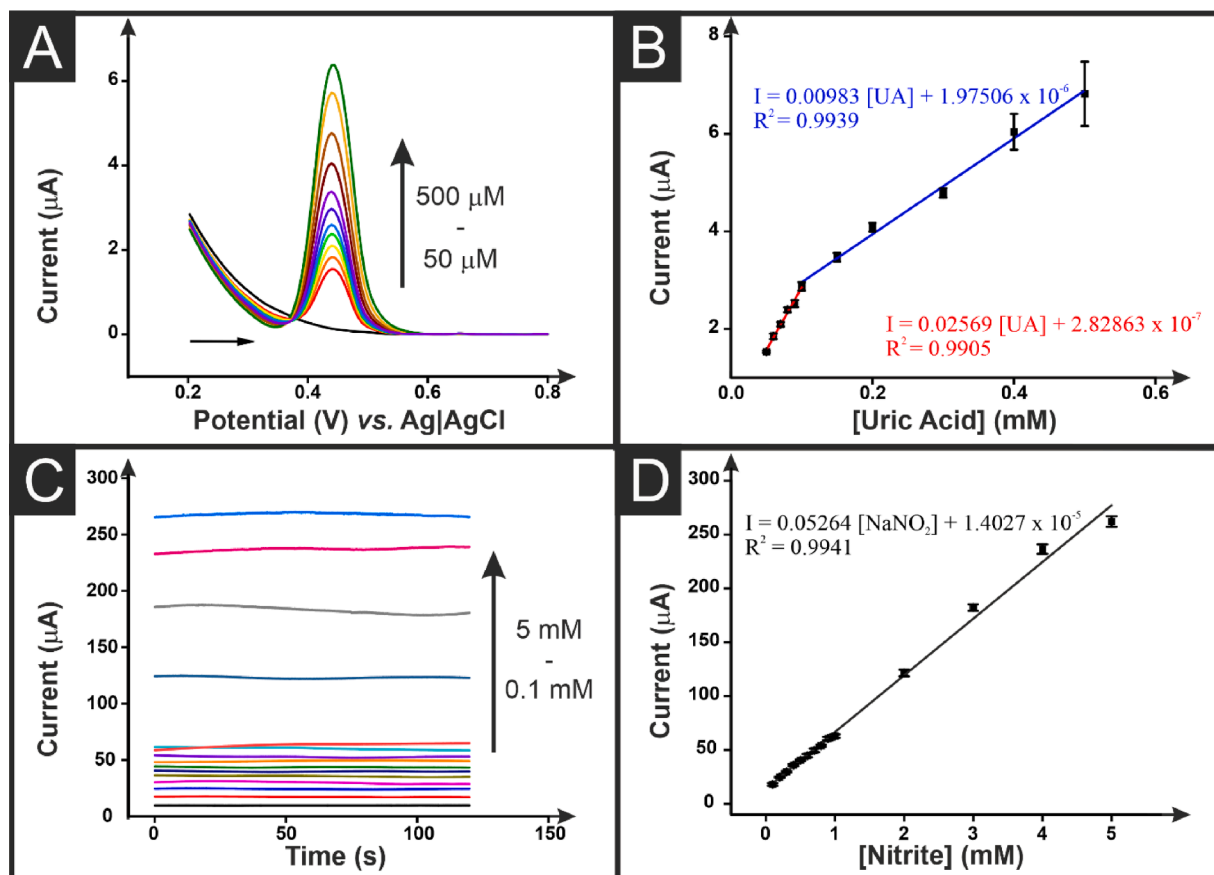


Fig. 6. (A) Differential pulse voltammograms of uric acid (30–500 μM) in synthetic urine using the rPETg additive manufactured electrode, nichrome wire counter electrode and Ag|AgCl reference electrode. Performed with a step potential of 5 mV, amplitude of 25 mV, modulation time of 50 s, and interval time of 0.5 s. (B) Calibration plot corresponding to the detection of uric acid (30–500 μM) in synthetic urine using the rPETg additive manufactured electrode, nichrome wire counter electrode and Ag|AgCl reference electrode. (C) Chronoamperograms for the detection of sodium nitrite (0.1–5 mM) in synthetic urine using the rPETg additive manufactured electrode, nichrome wire counter electrode and Ag|AgCl reference electrode. (D) Calibration plot corresponding to the detection of sodium nitrite (0.1–5 mM) in synthetic urine using the rPETg additive manufactured electrode, nichrome wire counter electrode and Ag|AgCl reference electrode.

then presented in Fig. 6C, with the corresponding linear calibration plot shown in Fig. 6D. In this case a sensitivity of $52.6 \mu\text{A mM}^{-1}$ was observed with a LOQ of $8.97 \mu\text{M}$ and a LOD of $2.69 \mu\text{M}$. These results clearly show the applicability of these sterilised rPETg additive manufactured electrodes toward the use as sensing platforms within biological samples. The ability for electrodes printed from these materials to be sterilised successfully through two different methodologies without impacting their electrochemical performance, alongside the added benefit of lower solution ingress offers great promise for use as healthcare sensors in the future. In addition, the production of these materials from recycled plastic sources, and the reproducibility of results obtained over up to 10 measurements could not only introduce significant cost savings but also help to tackle excessive plastic waste, which are both prevalent issues in healthcare today.

4. Conclusions

In this work we report the production of an electrically conductive additive manufacturing filament using 67 wt% recycled PETg, 11 wt% carbon black, 11 wt% multi-walled carbon nanotubes, and 11 wt% graphene nanoplatelets. This filament showed improved conductivity and electrochemical performance against the near-ideal outer sphere redox probe $[\text{Ru}(\text{NH}_3)_6]^{3+/2+}$ when compared to previously reported conductive rPETg and the commercially available PLA benchmark. To further improve the electrochemical performance of the conductive rPETg against inner-sphere probes, the activation of the additive manufactured electrodes post-print was optimised, with the best

performance reached after mechanically polishing the electrode followed by electrochemical activation within aqueous sodium hydroxide.

To test the additive manufactured electrodes printed from this conductive rPETg toward use as healthcare sensors, the electrodes were first sterilised through the application of UV light, which was shown to have no effect on the electrochemical performance, unlike for the commercial conductive PLA filament. The rPETg electrodes were then applied to the successful detection of uric acid and sodium nitrite within synthetic urine samples. Using differential pulse voltammetry, uric acid was determined within synthetic urine with a sensitivity of $25.7 \mu\text{A} \mu\text{M}^{-1}$, a LOQ $0.92 \mu\text{M}$ and, a LOD of $0.27 \mu\text{M}$. Utilising chronoamperometry, the additive manufactured electrodes then successfully detected nitrite within synthetic urine with a sensitivity of $52.6 \mu\text{A} \text{mM}^{-1}$, LOQ of $8.97 \mu\text{M}$ and LOD of $2.69 \mu\text{M}$. The re-useability of the electrodes was also tested for the detection of uric acid, showing that the electrode could be used up to 10 times before a significant decrease in the results was obtained. This work shows that conductive rPETg has a prominent place within the development of additive manufactured electrochemical healthcare sensors due to its high-performance, ability to be sterilised, ability to be re-used, low solution ingress, and its ability to tackle rising costs and plastic waste problems within the healthcare sector.

CRedit authorship contribution statement

Jéssica R. Camargo: Writing – review & editing, Writing – original draft, Methodology, Investigation, Formal analysis, Data curation.

Robert D. Crapnell: Writing – review & editing, Writing – original draft, Supervision, Methodology, Investigation, Formal analysis, Data curation, Conceptualization. **Elena Bernalte:** Writing – review & editing, Writing – original draft, Supervision, Methodology, Investigation, Formal analysis, Data curation, Conceptualization. **Alexander J. Cunliffe:** Methodology, Investigation. **James Redfern:** Methodology, Investigation. **Bruno C. Janegitz:** Writing – review & editing, Writing – original draft, Supervision, Methodology, Investigation, Funding acquisition. **Craig E. Banks:** Writing – review & editing, Writing – original draft, Supervision, Resources, Project administration, Methodology, Investigation, Funding acquisition, Formal analysis, Data curation, Conceptualization.

Declaration of competing interest

The authors declare that they have no known competing financial interests or personal relationships that could have appeared to influence the work reported in this paper.

Data availability

Data will be made available on request.

Acknowledgments

The authors thank the financial support provided by Fundação de Amparo à Pesquisa do Estado de São Paulo (FAPESP, 2023/06793-4 and 2023/00321-3) and Conselho Nacional de Desenvolvimento Científico e Tecnológico (CNPq 301796/2022-0). We thank EPSRC for funding (EP/W033224/1).

Supplementary materials

Supplementary material associated with this article can be found, in the online version, at [doi:10.1016/j.apmt.2024.102285](https://doi.org/10.1016/j.apmt.2024.102285).

References

- M. Attaran, The rise of 3-D printing: The advantages of additive manufacturing over traditional manufacturing, *Bus. Horiz.* 60 (5) (2017) 677.
- R.M. Cardoso, et al., Additive-manufactured (3D-printed) electrochemical sensors: A critical review, *Anal. Chim. Acta* 1118 (2020) 73.
- A. Abdalla, B.A. Patel, 3D-printed electrochemical sensors: A new horizon for measurement of biomolecules, *Curr. Opin. Electrochem.* 20 (2020) 78.
- A. Ambrosi, M. Pumera, 3D-printing technologies for electrochemical applications, *Chem. Soc. Rev.* 45 (10) (2016) 2740.
- A.G.-M. Ferrari, et al., Exploration of defined 2-dimensional working electrode shapes through additive manufacturing, *Analyst* 147 (22) (2022) 5121.
- M.J. Whittingham, et al., Additively manufactured rotating disk electrodes and experimental setup, *Anal. Chem.* 94 (39) (2022) 13540.
- M.J. Whittingham, et al., Additive manufacturing for electrochemical labs: An overview and tutorial note on the production of cells, electrodes and accessories, *Talanta Open* 4 (2021) 100051.
- C.W. Foster, et al., 3D printed graphene based energy storage devices, *Sci. Rep.* 7 (1) (2017) 42233.
- K. Ghosh, M. Pumera, MXene and MoS₃-x Coated 3D-Printed Hybrid Electrode for Solid-State Asymmetric Supercapacitor, *Small Methods* 5 (8) (2021) 2100451.
- K. Ghosh, M. Pumera, Free-standing electrochemically coated MoS_x based 3D-printed nanocarbon electrode for solid-state supercapacitor application, *Nanoscale* 13 (11) (2021) 5744.
- M.P. Browne, et al., 3D printing for electrochemical energy applications, *Chem. Rev.* 120 (5) (2020) 2783.
- R.D. Crapnell, et al., All-in-One Single-Print Additively Manufactured Electroanalytical Sensing Platforms, *ACS Meas. Sci. Au* 2 (2) (2021) 167.
- H.M. Elbardisy, et al., Versatile additively manufactured (3D printed) wall-jet flow cell for high performance liquid chromatography-amperometric analysis: application to the detection and quantification of new psychoactive substances (NBOMes), *Anal. Methods* 12 (16) (2020) 2152.
- L.V. de Faria, et al., Cyclic square-wave voltammetric discrimination of the amphetamine-type stimulants MDA and MDMA in real-world forensic samples by 3D-printed carbon electrodes, *Electrochim. Acta* 429 (2022) 141002.
- B.C. Janegitz, et al., Novel Additive Manufactured Multielectrode Electrochemical Cell with Honeycomb Inspired Design for the Detection of Methyl Parathion in Honey Samples, *ACS Meas. Sci. Au* 3 (3) (2023) 217–225.
- J. Muñoz, M. Pumera, Accounts in 3D-printed electrochemical sensors: towards monitoring of environmental pollutants, *ChemElectroChem* 7 (16) (2020) 3404.
- E. Redondo, et al., 3D-printed nanocarbon sensors for the detection of chlorophenols and nitrophenols: Towards environmental applications of additive manufacturing, *Electrochem. Commun.* 125 (2021) 106984.
- C. Kalinke, et al., Sensing of L-methionine in biological samples through fully 3D-printed electrodes, *Anal. Chim. Acta* 1142 (2021) 135.
- C. Kalinke, et al., 3D-printed immunosensor for the diagnosis of Parkinson's disease, *Sens. Actuators B Chem.* 381 (2023) 133353.
- C. Kalinke, et al., Prussian blue nanoparticles anchored on activated 3D printed sensor for the detection of L-cysteine, *Sens. Actuators B Chem.* 362 (2022) 131797.
- R.D. Crapnell, et al., Additive manufacturing electrochemistry: an overview of producing bespoke conductive additive manufacturing filaments, *Mater. Today* 71 (2023) 73–90.
- K. Ghosh, et al., 2D MoS₂/carbon/poly(lactic acid) filament for 3D printing: Photo and electrochemical energy conversion and storage, *Appl. Mater. Today* 26 (2022) 101301.
- P. Wuamprakhon, et al., Recycled Additive Manufacturing Feedstocks for Fabricating High Voltage, Low-Cost Aqueous Supercapacitors, *Adv. Sustain. Syst.* 7 (2) (2023) 2200407.
- J.P. Hughes, et al., Single step additive manufacturing (3D printing) of electrocatalytic anodes and cathodes for efficient water splitting, *Sustain. Energy Fuels* 4 (1) (2020) 302.
- I.V. Arantes, et al., Mixed graphite/carbon black recycled PLA conductive additive manufacturing filament for the electrochemical detection of oxalate, *Anal. Chem.* 95 (40) (2023) 15086.
- I.V. Arantes, et al., Additive manufacturing of a portable electrochemical sensor with a recycled conductive filament for the detection of atropine in spiked drink samples, *ACS Appl. Eng. Mater.* 1 (9) (2023) 2397.
- R.D. Crapnell, et al., Multi-walled carbon nanotubes/carbon black/rPLA for high-performance conductive additive manufacturing filament and the simultaneous detection of acetaminophen and phenylephrine, *Microchim. Acta* 191 (2) (2024) 96.
- C. Kalinke, et al., Recycled additive manufacturing feedstocks with carboxylated multi-walled carbon nanotubes toward the detection of yellow fever virus cDNA, *Chem. Eng. J.* 467 (2023) 143513.
- L.R.G. Silva, et al., Additive manufacturing of carbon black immunosensors based on covalent immobilization for portable electrochemical detection of SARS-CoV-2 spike S1 protein, *Talanta Open* 8 (2023) 100250.
- L.R.G. Silva, et al., 3D electrochemical device obtained by additive manufacturing for sequential determination of paraquat and carbendazim in food samples, *Food Chem.* 406 (2023) 135038.
- J.S. Stefano, et al., New carbon black-based conductive filaments for the additive manufacture of improved electrochemical sensors by fused deposition modeling, *Microchim. Acta* 189 (11) (2022) 414.
- E. Sigley, et al., Circular economy electrochemistry: creating additive manufacturing feedstocks for caffeine detection from post-industrial coffee pod waste, *ACS Sustain. Chem. Eng.* 11 (7) (2023) 2978.
- R.D. Crapnell, et al., Circular Economy Electrochemistry: Recycling Old Mixed Material Additively Manufactured Sensors into New Electroanalytical Sensing Platforms, *ACS Sustain. Chem. Eng.* 11 (24) (2023) 9183–9193.
- R.D. Crapnell, et al., Utilising bio-based plasticiser castor oil and recycled PLA for the production of conductive additive manufacturing feedstock and detection of bisphenol A, *Green Chem.* 25 (2023) 5591–5600.
- C. Kalinke, et al., Influence of filament aging and conductive additive in 3D printed sensors, *Anal. Chim. Acta* 1191 (2022) 339228.
- R.J. Williams, et al., The effect of water ingress on additively manufactured electrodes, *Mater. Adv.* 3 (20) (2022) 7632.
- K.S. Erokhin, et al., Revealing interactions of layered polymeric materials at solid-liquid interface for building solvent compatibility charts for 3D printing applications, *Sci. Rep.* 9 (1) (2019) 20177.
- I.M. Alarifi, PETG/carbon fiber composites with different structures produced by 3D printing, *Polym. Test.* 120 (2023) 107949.
- S.S. Bedi, et al., Thermal characterization of 3D printable multifunctional graphene-reinforced polyethylene terephthalate glycol (PETG) composite filaments enabled for smart structural applications, *Polym. Eng. Sci.* 63 (9) (2023) 2841.
- M.H. Hassan, et al., The potential of polyethylene terephthalate glycol as biomaterial for bone tissue engineering, *Polymers (Basel)* 12 (12) (2020) 3045.
- C. Yan, et al., PETG: Applications in Modern Medicine, *Eng. Regen.* 5 (1) (2024) 45.
- R.D. Crapnell, et al., Recycled PETg embedded with graphene, multi-walled carbon nanotubes and carbon black for high-performance conductive additive manufacturing feedstock, *RSC Adv.* 14 (12) (2024) 8108.
- E. Bernalte, et al., The Effect of Slicer Infill Pattern on the Electrochemical Performance of Additively Manufactured Electrodes, *ChemElectroChem* 11 (4) (2024) e202300576.
- E.M. Richter, et al., Complete additively manufactured (3D-printed) electrochemical sensing platform, *Anal. Chem.* 91 (20) (2019) 12844.
- G. Greczynski, L. Hultman, The same chemical state of carbon gives rise to two peaks in X-ray photoelectron spectroscopy, *Sci. Rep.* 11 (1) (2021) 1.
- M. Wen, et al., The electrical conductivity of carbon nanotube/carbon black/polypropylene composites prepared through multistage stretching extrusion, *Polymer* 53 (7) (2012) 1602.

- [47] C. Kalinke, et al., Comparison of activation processes for 3D printed PLA-graphene electrodes: electrochemical properties and application for sensing of dopamine, *Analyst* 145 (4) (2020) 1207.
- [48] D.P. Rocha, et al., Posttreatment of 3D-printed surfaces for electrochemical applications: A critical review on proposed protocols, *Electrochem. Sci. Adv.* 2 (5) (2022) e2100136.
- [49] T. Chen, et al., Photodegradation behavior and mechanism of poly (ethylene glycol-co-1, 4-cyclohexanedimethanol terephthalate)(PETG) random copolymers: Correlation with copolymer composition, *RSC adv.* 6 (104) (2016) 102778.
- [50] R. Blume, et al., Characterizing graphitic carbon with X-ray photoelectron spectroscopy: a step-by-step approach, *ChemCatChem* 7 (18) (2015) 2871.
- [51] T.R. Gengenbach, et al., Practical guides for x-ray photoelectron spectroscopy (XPS): Interpreting the carbon 1s spectrum, *J. Vac. Sci. Technol. A* 39 (1) (2021) 013204.
- [52] R.D. Crapnell, C.E. Banks, Perspective: What constitutes a quality paper in electroanalysis? *Talanta Open* 4 (2021) 100065.
- [53] J.S. Stefano, et al., New conductive filament ready-to-use for 3D-printing electrochemical (bio)sensors: Towards the detection of SARS-CoV-2, *Anal. Chim. Acta* 1191 (2022) 339372.
- [54] R.M. Cardoso, et al., 3D-Printed graphene/poly(lactic acid) electrode for bioanalysis: Biosensing of glucose and simultaneous determination of uric acid and nitrite in biological fluids, *Sens. Actuators B Chem.* 307 (2020) 127621.